RESEARCH PAPER

Amelioration of renal ischaemia–reperfusion injury by liposomal delivery of curcumin to renal tubular epithelial and antigen-presenting cells

NM Rogers[1,2,3,4], MD Stephenson[1,4], AR Kitching[5], JD Horowitz[3,4] and PTH Coates[1,2,3,5]

[1]Transplant Immunology Laboratory, Hanson Institute, Adelaide, SA, Australia, [2]Central Northern Adelaide Renal and Transplantation Service, Royal Adelaide Hospital, Adelaide, SA, Australia, [3]Department of Medicine, The University of Adelaide, Adelaide, SA, Australia, [4]Basil Hetzel Institute for Medical Research, The Queen Elizabeth Hospital, Woodville, SA, Australia, [5]Centre for Inflammatory Diseases, Monash University Department of Medicine, Monash Medical Centre, Clayton, Vic., Australia, and [6]Centre for Stem Cell Research, The University of Adelaide, Adelaide, SA, Australia

BACKGROUND AND PURPOSE

Renal ischaemia–reperfusion (IR) injury is an inevitable consequence of renal transplantation, causing significant graft injury, increasing the risk of rejection and contributing to poor long-term graft outcome. Renal injury is mediated by cytokine and chemokine synthesis, inflammation and oxidative stress resulting from activation of the NF-κB pathway.

EXPERIMENTAL APPROACH

We utilized liposomal incorporation of a potent inhibitor of the NF-κB pathway, curcumin, to target delivery to renal tubular epithelial and antigen-presenting cells. Liposomes containing curcumin were administered before bilateral renal ischaemia in C57/B6 mice, with subsequent reperfusion. Renal function was assessed from plasma levels of urea and creatinine, 4 and 24 h after reperfusion. Renal tissue was examined for NF-κB activity and oxidative stress (histology, immunostaining) and for apoptosis (TUNEL). Cytokines and chemokines were measured by RT-PCR and Western blotting.

KEY RESULTS

Liposomal curcumin significantly improved serum creatinine, reduced histological injury and cellular apoptosis and lowered Toll-like receptor-4, heat shock protein-70 and TNF-α mRNA expression. Liposomal curcumin also reduced neutrophil infiltration and diminished inflammatory chemokine expression. Curcumin liposomes reduced intracellular superoxide generation and increased superoxide dismutase levels, decreased inducible NOS mRNA expression and 3-nitrotyrosine staining consistent with limitations in nitrosative stress and inhibited renal tubular mRNA and protein expression of thioredoxin-interacting protein. These actions of curcumin were mediated by inhibition of NF-κB, MAPK and phospho-S6 ribosomal protein.

CONCLUSIONS AND IMPLICATIONS

Liposomal delivery of curcumin promoted effective, targeted delivery of this non-toxic compound that provided cytoprotection via anti-inflammatory and multiple antioxidant mechanisms following renal IR injury.

Abbreviations

APC, antigen-presenting cells; DHE, dihydroethidium; HSP, heat shock protein; iNOS, inducible NOS; IR, ischaemia–reperfusion; ROS, reactive oxygen species; SOD, superoxide dismutase; TEC, tubular epithelial cells; TLR, toll-like receptor; TXNIP, thioredoxin-interacting protein

Introduction

Renal ischaemia–reperfusion injury (IR injury) is a significant cause of acute and end-stage kidney disease, producing serious morbidity and mortality and prolonged hospitalization (Preston and Epstein, 1997). IR injury also occurs during the obligatory interruption of blood flow and haemodynamic changes during the peri-operative kidney transplant period. It remains an important initiator of acute renal transplant rejection (Halloran *et al.*, 1997) and delayed allograft function (Shoskes and Halloran, 1996; Hetzel *et al.*, 2002) and a factor in long-term graft survival (Feldman *et al.*, 1996). IR injury also contributes to kidney dysfunction in a variety of clinical settings, from cardiovascular surgery to septicaemia. Acute ischaemia leads to depletion of adenosine triphosphate, inducing tubular epithelial cell (TEC) injury and hypoxic cell death. Restoration of blood flow causes a paradoxical increase in injury by promoting leukocyte activation and infiltration, cytokine production and reactive oxygen species (ROS) generation.

Multiple stimuli, including hypoxia and ROS, activate the NF-κB pathway in IR injury, playing a central role in the regulation of numerous and deleterious downstream pathways (Donnahoo *et al.*, 2000; Tsoulfas and Geller, 2001). These targets include complement, pro-inflammatory cytokines (IL-6, TNF-α) and their receptors, inflammatory mediators (inducible NOS, iNOS) and leukocyte adhesion molecules. TEC are primarily affected, producing parenchymal injury mediated by both Toll-like receptors (TLR)-2 and TLR-4 (Leemans *et al.*, 2005; Boros and Bromberg, 2006), although resident renal dendritic cells are the predominant source of cytokines (Dong *et al.*, 2007). New therapeutic strategies that target NF-κB in both TEC and antigen-presenting cells (APC) inhibiting the inflammatory and innate immune cascades responsible for amplification of injury are potential effective treatments or prevention of IR injury.

Curcumin [diferuloylmethane, 1,7-bis(4-hydroxy-3-methoxiphenyl)-1,6-heptadiene-3,5-dione)] is a polyphenol compound derived from the plant *Curcuma longa* (turmeric). Curcumin exhibits antioxidant (Balasubramanyam *et al.*, 2003, Ruby *et al.*, 2003), anti-inflammatory (Yadav *et al.*, 2005), antimicrobial (Apisariyakul *et al.*, 1995; Mazumder *et al.*, 1995; Negi *et al.*, 1999), anti-proliferative (Garg *et al.*, 2005) and immunomodulatory (Rogers *et al.*, 2010b) effects and thus has therapeutic potential in IRI. Curcumin is water-insoluble (Jagetia and Aggarwal, 2007) with a high octanol : water partition coefficient (logP$_{ow}$ = 3.29), limiting its utility as an orally administered agent. Previous studies assessing the effect of curcumin on animal models of ir injury have employed oral administration with minor functional salvage (Bayrak *et al.*, 2008), or direct infusion into the vascular tree (Shen *et al.*, 2007), which has limited clinical applicability. The lipid solubility of curcumin lends itself to liposomal incorporation, facilitating delivery *in vivo*.

In the current study, the potential for liposomal curcumin to be delivered to the renal parenchyma is explored, and the hypothesis that liposomal curcumin is protective in a model of renal IR injury is tested. Furthermore, the mechanisms underlying putative cytoprotection are evaluated.

Methods

Mice

All animal care and experimental procedures were approved by the institutional Animal Ethics Committee. We used 7–8 week old male C57BL/6 mice, housed in pathogen-free conditions at the Animal Care Facility at the Institute of Medical and Veterinary Science (Adelaide, Australia).

Liposome formulation

Liposomes containing curcumin were prepared by thin film hydration. Briefly, 100 mg egg phosphatidylcholine (Avanti Lipids, Alabaster, AL) and 3.5 mg curcumin (Sigma Aldrich, St Louis, MO) were dissolved in 9 ml chloroform and 1 ml 100% ethanol respectively. The solutions were mixed and the solvents evaporated using a rotary evaporator (Buchi, Flawil, Switzerland) at room temperature, under reduced pressure. Liposomes were re-dispersed in 2 ml HEPES buffer (Amresco, Solon, OH) and extruded through 400 nm polycarbonate membranes (Whatman, Kent, UK) under a stream of nitrogen. For some experiments, liposomes were fluorescently labelled by adding ethanolic stock solution (10mg/ml) of 1,1′-dioctadecyl-3,3,3′,3′-tetramethylindocarbocyanine perchlorate (DiI; Molecular Probes, Eugene, OR) following extrusion, to give 0.1mg DiI per µL liposome.

In vivo *fate of liposomes*

One hundred and fifty microlitres (150 µL) of liposome was injected i.v. into C57BL/6 mice. Twenty-four hours later, kidneys were removed and digested with Collagenase D (Roche, Basel, Switzerland). Cell suspensions were stained for 20 min in the dark at 4°C with anti-mouse MHC FITC, CD11c FITC or PE-CY7, CD8α APC, B220 PE-CY5 or F480 PE-CY5, PDCA-1 FITC (all Biolegend, San Diego, CA) then fixed at room temperature with 10% FACS-lysing solution (BD PharMingen, San Diego, CA) and washed in staining buffer. Flow cytometry was performed in a FACSCanto flow cytometer and analysed using FACSDiva software (v6.3.1, BD PharMingen).

Confocal microscopy

Kidneys from C57BL/6 mice, untreated or injected with DiI-labelled liposomes, were collected, embedded in OCT compound and snap frozen in liquid nitrogen. Sections were fixed in ice-cold acetone (Sigma Aldrich) for 5 min, dried at room temperature and stained with 4′,6-diamidino-2-phenylindole (DAPI). Slides were washed twice in PBS, mounted with mounting medium (DAKO, Glostrup, Denmark) and imaged on an Apotome microscope (Zeiss, Oberkochen, Germany).

Staining for NF-κB

Renal APC were isolated from male C57BL/6 mice 12 h after injection with 150 µL liposome (curcumin or vehicle control). Briefly, kidneys were dissected and digested with collagenase D (Roche) and DNase (Roche). Cells were washed in PBS, and the supernatant filtered through a 70 µm cell strainer. RBC lysis was performed using an appropriate buffer. The remaining cell population was incubated overnight in complete media in Lab-Tek® chamber slides (Nunc Nalge

International, Rochester, NY) and then treated *ex vivo* with or without LPS (1 µg·µL^{-1}, Sigma Aldrich) for 6 h. Slides were washed twice with PBS, and the adherent cells were subsequently stained with polyclonal rabbit NF-κB-p50 antibody (Santa Cruz Biotechnology, Santa Cruz, CA), goat anti-rabbit IgG FITC (Santa Cruz Biotechnology) and DAPI. Confocal microscopy was performed, and the density of nuclear NF-κB-p50 staining was assessed using ImageJ (NIH, Bethesda, MD, USA) in 20 cells each from three individual experiments.

Kidney tissue was sectioned at 4 µm, underwent standard antigen retrieval and stained for NF-κB-p65 (Cell Signaling, Boston, MA) followed by 3,3'-diaminobenzidine (DAB) substrate-chromogen solution (Dako, Glostrup, Denmark). Renal TEC demonstrating nuclear staining for phospho-NF-κB-p65 were counted in 10 randomly selected corticomedullary fields at 40× magnification.

IR injury

Mice (*n* = 10–12 per group) were injected i.v. with 150 µL empty liposome (vehicle control) or curcumin liposome, 12 h before IRI. The administered dose of curcumin was 4 mg·kg^{-1}. Mice were anaesthetized using isoflurane and oxygen titrated to effect, and body temperature was maintained at 37°C. A midline laparotomy incision was made, and microaneurysm clips occluded both renal pedicles for 30 min. Animals received 600 µL 0.9% saline and 0.4 mg·kg^{-1} buprenorphine s.c. at the end of the procedure. Sham-operated mice were subjected to liposome injection, anaesthesia and midline laparotomy only.

Assessment of renal function after IR injury

Renal function was assessed by measurement of plasma urea and creatinine 4 or 24 h after IR injury using the urease method (OSR 6141, Beckman Coulter, Brea, CA) and a Jaffe creatine picric acid reaction (OSR 6178, Beckman Coulter) analysed on a Beckman Coulter 680 or an Olympus AU640 analyser respectively (Beckman Coulter).

Kidney histology

Histological examination to detect tubular vacuolization, infarction and cast formation was performed independently on Periodic Acid–Schiff (PAS)-stained sections by a nephrologist and a renal pathologist unaware of treatment groups. Renal injury scores were determined by the percentage of field involved (0–10% = 0, 10–25% = 1, 25–50% = 2, 50–75% = 3, >75% = 4) for assessment of three randomly selected corticomedullary fields in three separate sections from each mouse (magnification 200×). Intrarenal neutrophil infiltration was quantitated by manual counting of polymorphonuclear cells in 10 randomly chosen corticomedullary fields (magnification 400×).

Renal parenchymal cellular apoptosis

Terminal transferase dUTP nick-end-labelling (TUNEL) staining was used to detect apoptosis with a commercially available *in situ* cell death detection kit (Roche), performed according to manufacturer's instruction.

Oxidative fluorescent microscopy

Dihydroethidium (DHE, Axxora San Diego, CA, USA) was used to evaluate *in situ* production of superoxide. DHE (10 µM) was applied to unfixed frozen sections each section, incubated in a light-protected humidified chamber at 37°C for 30 min, washed with PBS and mounted with fluorescent mounting medium (Dako). Images were obtained with a Zeiss Apotome microscope.

RNA extraction and quantification by real-time PCR

Total RNA was extracted using Qiagen RNeasy® Mini Kits (Qiagen, Hilden, Germany) as per the manufacturer's instructions. RNA was quantitated using the Experion® RNA Stdsens Analysis Kit (Bio-Rad Laboratories, Hercules, CA). Samples of RNA (1 µg) were reverse-transcribed as described previously (Rogers *et al.*, 2010b). PCR amplification was performed using a Rotor gene 3000 Real-time cycler (Corbett Research, Mortlake, Australia). Reactions were performed using AmpliTaq Gold® PCR Master Mix (Applied Biosystems, Scoresby, Australia), SYBR Green (Adelab, Thebarton, Australia), designed primers (Geneworks, Thebarton, Australia) and cDNA of template, standard, or non-template control. Results were run simultaneously with, and absolute copy number was normalized to the housekeeping gene hypoxanthine phosphoribosyltransferase 1 (HPRT1), analysed with Rotor-gene v5.0 (Corbett Research).

3-Nitrotyrosine and TXNIP immunofluorescent staining

Unfixed frozen sections were fixed with 4% paraformaldehyde for 5 min, washed in PBS and then blocked using 10% goat serum. Unconjugated 3-nitrotyrosine (1:250 dilution, Abcam, Cambridge, UK) or thioredoxin-interacting protein (TXNIP; 1:250 dilution, Santa Cruz Biotechnology) antibody was added and incubated for 2 h at room temperature. Sections were washed in PBS, incubated with goat anti-mouse AlexaFluor 488 (1:400 dilution, Molecular Probes) or FITC-conjugated goat anti-rabbit (1:400 dilution, Santa Cruz Biotechnology), respectively, for 1 h and then DAPI. Slides were washed in PBS, mounted with fluorescent mounting medium and imaged.

Western blotting

Kidney tissue was homogenized in 100 µL of lysis buffer (50 mM HEPES pH 7.4, 150 mM NaCl, 1% Triton X-100, 30 mM NaF, 10 mM Na$_4$P$_2$O$_7$, 10 mM EDTA, 1 µg·mL^{-1} each of aprotinin, antipain, pepstatin, leupeptin and benzamidine) and incubated on ice for 10 min. Protein was quantitated using a PierceΣ BCA protein Assay Kit (Thermo Scientific, Rockford, IL) according to the manufacturer's instructions, with BSA as a standard. Tissue extracts (10 µg of protein) were separated by SDS-PAGE, transferred onto a PVDF membrane and immunoblotted with pERK or pS6 ribosomal protein (1:1000 dilution, Cell Signaling, Danvers, MA), 3-nitrotyrosine antibody (1:4000 dilution, Abcam) or TXNIP antibody (1:200 dilution, Santa Cruz Biotechnology) followed by horse anti-mouse HRP secondary antibody (Cell Signalling). Novexâ chemiluminescent substrate (Invitrogen, Melbourne, Australia) was visualized using a LAS-4000 Luminescent Image Analyzer (Berthold, Bundoora, Australia).
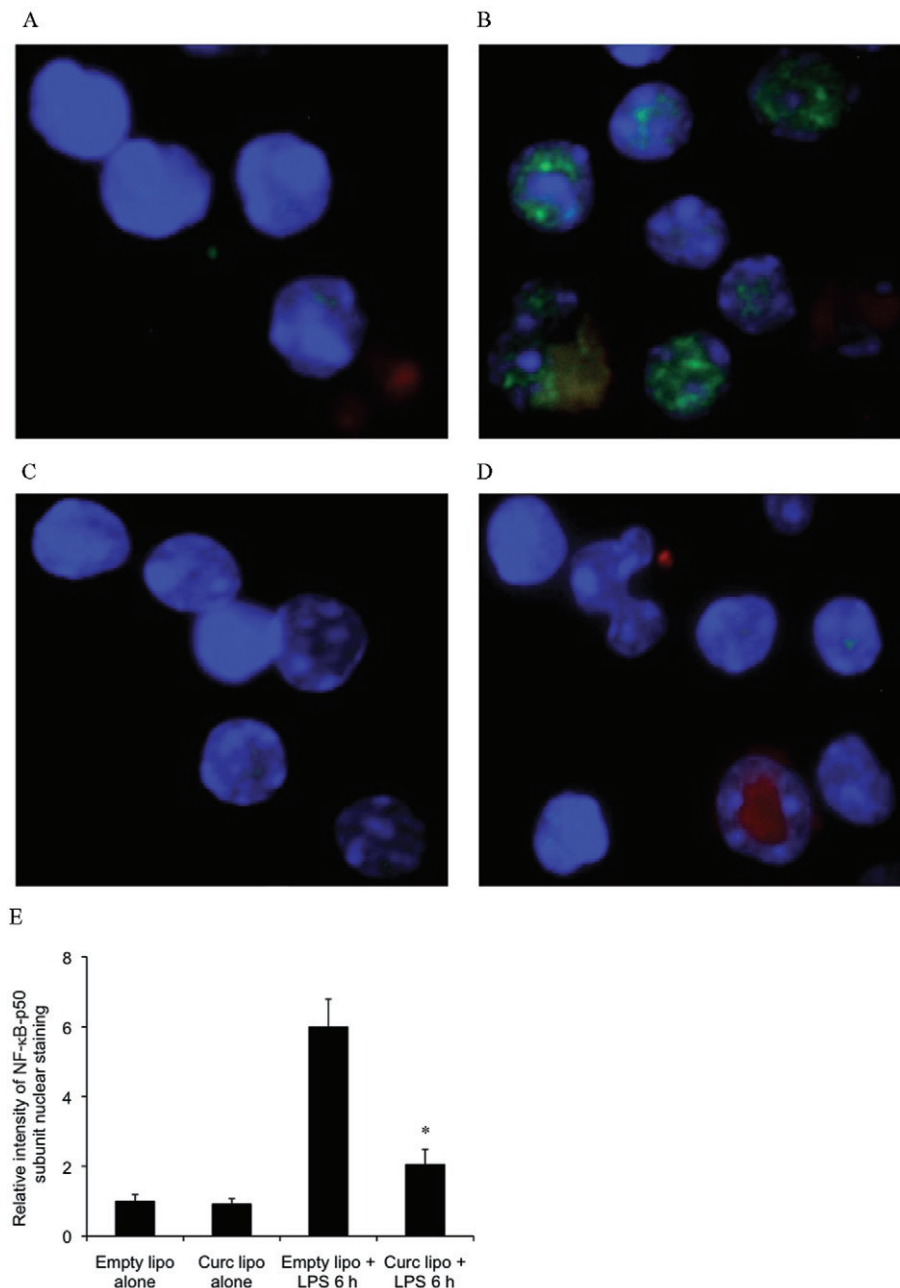
Figure 1

NF-κB activity is suppressed in renal APC of mice pre-treated with liposomal curcumin. (A–D) Liposomes were injected i.v. and renal APC were isolated 24 h later. After *ex vivo* incubation for 6 h with or without LPS, APC were fixed and analysed by confocal microscopy at 40× resolution. APC from mice pretreated with liposomal curcumin failed to up-regulate NF-κB-p50 in response to a maturation stimulus. Cell nuclei are blue, DiI-labelled liposomes are red and NF-κB-p50 is green. Results are representative of four independent experiments. (E) Graphical representation of relative intensity of nuclear NF-κB-p50 subunit staining. Results are representative of 20 cells from 4 independent experiments. Data are mean ± SEM of 10 mice per group. *$P < 0.05$, significantly different from control (empty lipo) and from liposomes alone (empty or curc).

Statistical analysis

The data is presented as mean ± SEM unless otherwise stated. Data were analysed with Student's *t*-test (parametric variables) or Mann–Whitney *U*-test (non-parametric variables) for means between two groups or ANOVA between multiple (>2) groups using STATA v11.0 (STATA Corporation, College Station, TX). In all cases, $P < 0.05$ was deemed significant.

Results

Liposomes are endocytosed by renal tubular and APC

To assess the cellular distribution of fluorescently labelled liposomes in the kidney 24 h after injection, tissue sections
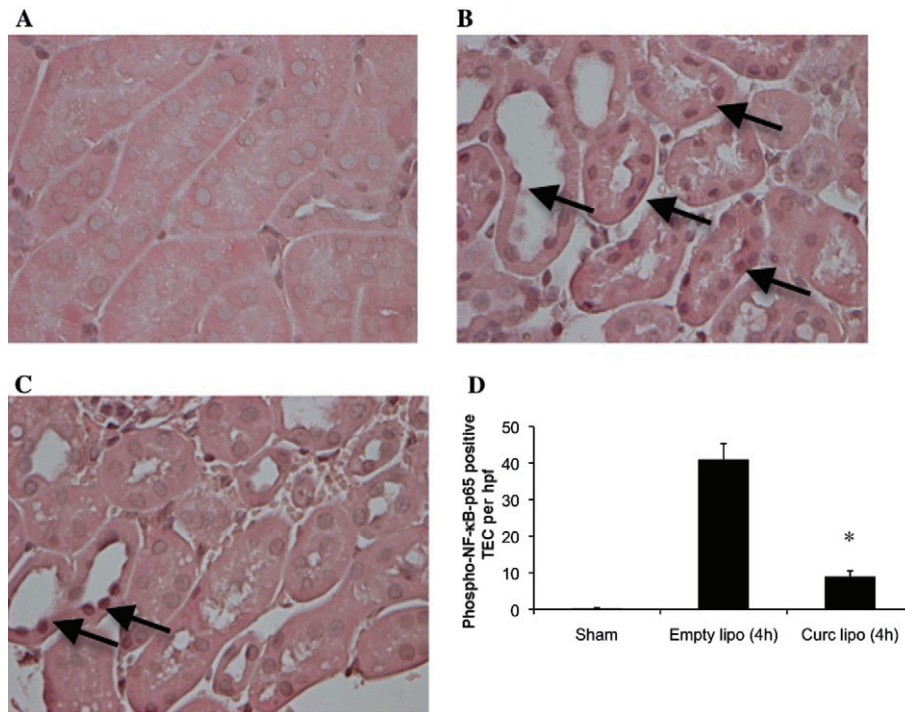
Figure 2

Liposomal curcumin limits NF-κB activation in renal TEC of mice following IR injury (IRI). Liposomes were injected i.v., and kidneys were isolated after 30 min ischaemia and 4 h reperfusion. Tissue sections were stained for phospho-NF-κB-p65 subunit. (A–C) Representative photomicrographs of corticomedullary sections illustrating phospho-NF-κB-p65 positive cells (arrows), representative of six sections per group (original magnification 400×). (D) Renal TEC nuclear staining for phospho NF-κB-p65 in control mice (empty liposome) was increased compared to mice pretreated with liposomal curcumin, confirmed by counting of positive cells per high-power field (hpf; 400× magnification). Data are mean ± SEM of 10 hpf from four mice per group. *$P < 0.01$, significantly different from Empty lipo and from sham.
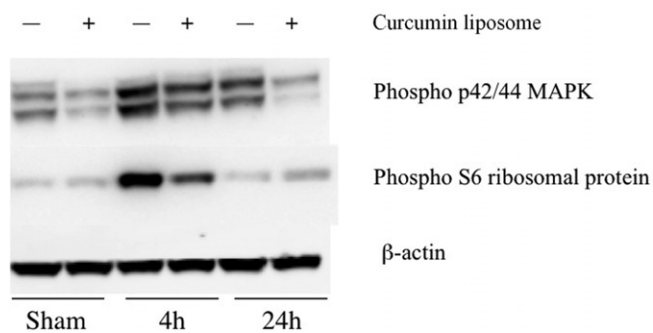

Figure 3

The effect of liposomal curcumin on MAPK and phospho-S6 ribosomal protein (pS6RP) pathways. Kidney tissue from mice treated with empty or curcumin liposomes were used for Western blot analysis of MAPK and pS6RP. Mice pretreated with liposomal curcumin demonstrated reduced MAPK p42/44 and pS6RP expression (the latter only at 4 h) compared with control mice. Results are representative of 3 independent experiments.

were examined by immunofluorescence, and cell suspensions of digested kidney were analysed by flow cytometry. DiI was chosen as the fluorescent label because of strong fluorescence, high lipophilic stability and lack of transfer between cell membranes once incorporated. Liposomal endocytosis by renal tubular epithelial cells (TEC) was confirmed by immunofluorescence microscopy (Supplemental Figure S1). Liposomes were also endocytosed by APC, including CD11c-CD11b+F480+ macrophages and subsets of CD11c+ myeloid and plasmacytoid dendritic cells (DC; Supplemental Figure S2).

Curcumin liposomes suppress NF-κB activity

The biological effect of curcumin is mediated by suppression of NF-κB activity, as extensively documented (Jobin et al., 1999; Kim et al., 2005, Yadav et al., 2005; Jagetia and Aggarwal, 2007; Capini et al., 2009; Rogers et al., 2010a). Activity of curcumin is maintained following liposomal incorporation (Lan et al., 2005; Wang et al., 2008; Capini et al., 2009), and this was confirmed in our study by semi-quantitative immunofluorescent staining for NF-κB-p50 subunit in renal APC, demonstrating failure of nuclear translocation in cells from curcumin liposome-injected mice, compared with controls (Figure 1). Liposomal curcumin also limited expression of phosphorylated NF-κB-p65 in renal TEC (Figure 2). Curcumin is not a specific inhibitor of NF-κB and has been shown to influence expression of additional transcription factors (Reddy and Aggarwal, 1994; Chen and Tan, 1998). Western blotting for phosphor-p42/44 MAPK (pERK) demonstrated
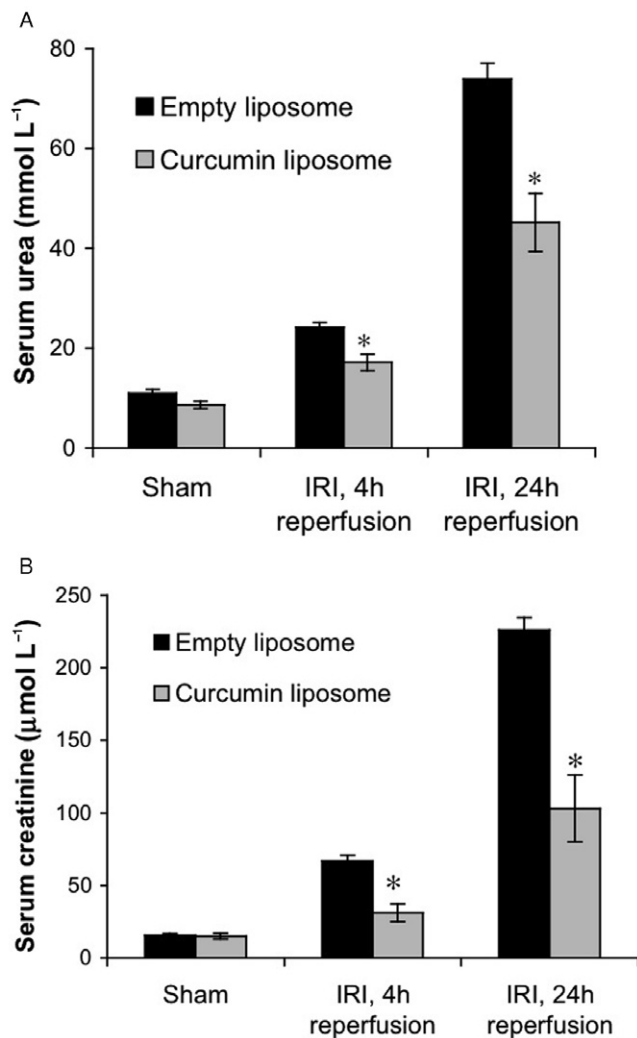
Figure 4

Liposomal curcumin improves renal function after IR injury (IRI). Renal function of mice pretreated with liposomal curcumin was improved compared with mice receiving vehicle control (empty liposomes) 4 and 24 h after renal IR injury (but not sham operation) as reflected by reduced (a) serum urea and (b) creatinine. Data are mean ± SEM of 10 mice per group. *P < 0.05, significant effect of curcumin liposomes.

Figure 5

Liposomal curcumin improves renal histology following IR injury (IRI). Scores for histological signs of renal injury were evaluated using PAS-stained renal tissue (as described in Methods). Tubular damage in corticomedullary regions, particularly (A) tubular vacuolization, (B) cast formation and (C) tubular infarction was significantly lower at 4 and 24 h after IRI, in mice receiving curcumin liposome compared with mice receiving vehicle control (empty liposomes), with no difference between sham operated animals. Data are mean ± SEM of 10 mice per group, three corticomedullary sections and two independent histopathological assessments per mouse. *P < 0.05, significant effect of curcumin liposomes. (D) Representative histological sections of corticomedullary tissue (original magnification 200×).

down-regulation at both reperfusion time points, and expression of phospho-S6 ribosomal protein (pS6RP) was reduced after 4 h of reperfusion in mice pre-treated with liposomal curcumin (Figure 3).

Liposomal curcumin reduced renal dysfunction following IR injury

To study the effect of curcumin liposomes on renal function after IR injury, serum urea and creatinine were measured at both 4 and 24 h after reperfusion. Mice pretreated with vehicle control (empty liposomes) showed significant renal dysfunction at both time points. Mice receiving curcumin
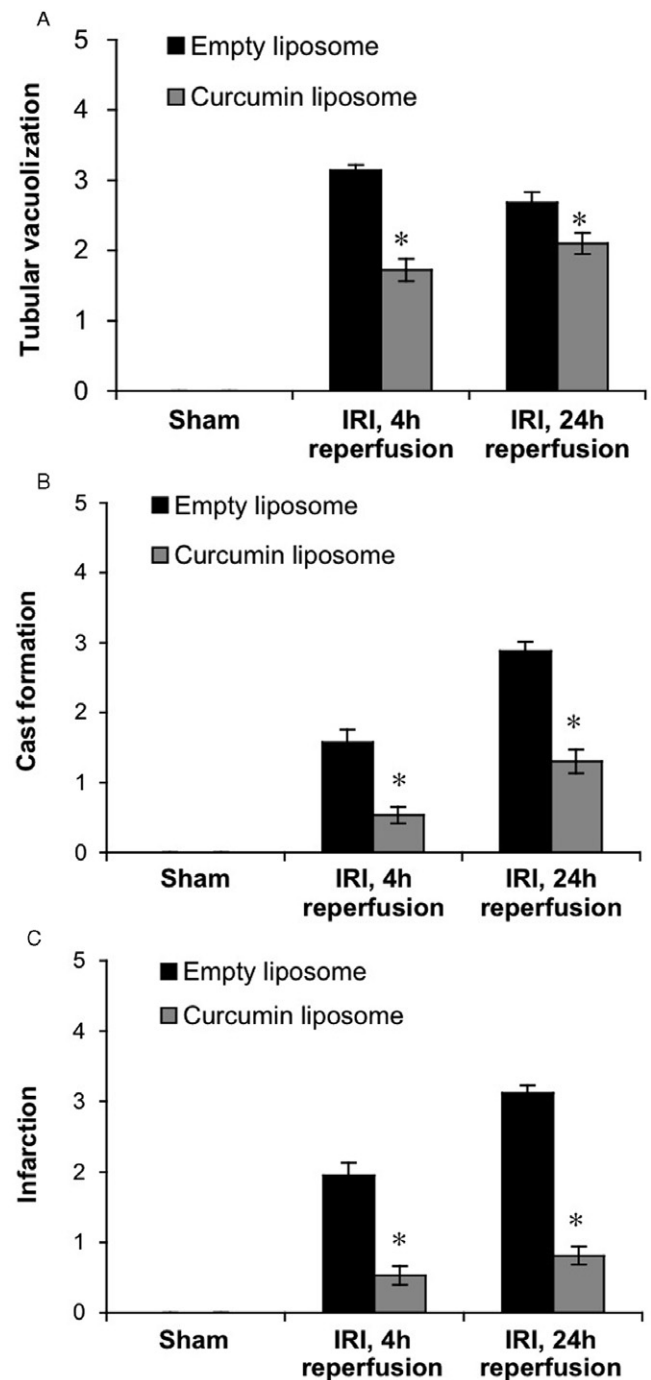
D

Empty liposome (vehicle control)

Sham 4h reperfusion 24h reperfusion

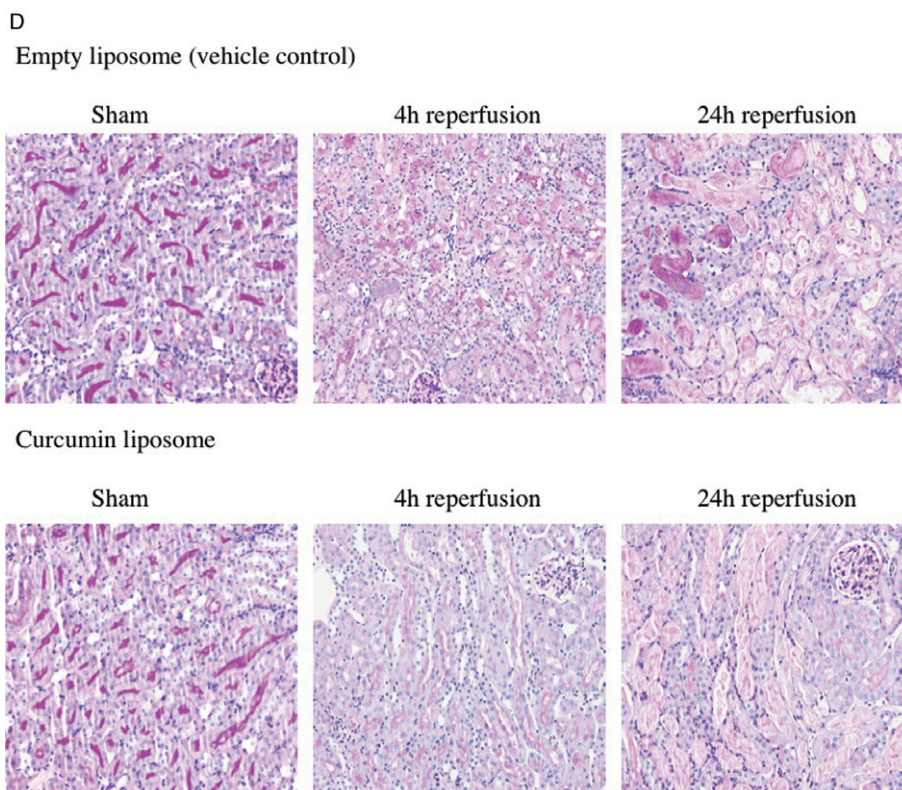Curcumin liposome

Sham 4h reperfusion 24h reperfusion

Figure 5
Continued.

liposomes were protected against acute renal failure as reflected by substantially lower serum urea and creatinine levels (Figure 4A,B).

Liposomal curcumin reduces renal tubular injury and apoptosis following IR injury

To determine the effects of liposomal curcumin on tubular injury, renal histology was evaluated. At both 4 and 24 h following reperfusion, ischaemic kidneys from control mice showed widespread tubular vacuolization, cast formation and tubular infarction (Figure 5A–C). Kidneys from curcumin-treated mice displayed reductions in tubular damage when directly compared with kidneys of control mice. However, tubular vacuolization was decreased at 24 h reperfusion in control mice compared with the curcumin-treated cohort. This was likely due to a substantial increase in tissue infarction and TEC necrosis seen at this time, in control mice.

Renal IR injury is also characterized by widespread cellular apoptosis. Curcumin has recognized cytoprotective characteristics but may induce apoptosis and micronucleation (Choudhuri *et al.*, 2002; Agwarwal *et al.*, 2003). To confirm that liposomal curcumin did not induce apoptosis, TUNEL staining was used to assess cellular apoptosis. Compared with sham-operated animals, mice subjected to bilateral IR injury demonstrated significant apoptosis within 4 h, and this was not increased after 24 h reperfusion, presumably due to

extensive cellular necrosis (Figure 6A,B). Notably, the number of apoptotic cells in kidneys from mice receiving liposomal curcumin was markedly lower at both reperfusion time points.

Liposomal curcumin reduces pro-inflammatory cytokine and chemokine expression following IR injury

Production of pro-inflammatory mediators is linked with the severity of renal structural and functional disturbance following IR injury. The increased expression of TLR4 was prevented in mice receiving curcumin liposomes (Figure 7A), in keeping with previous studies demonstrating up-regulation in renal IR injury (Wu *et al.*, 2007). HSP70, an endogenous factor for protecting intracellular protein integrity, was significantly attenuated in mice treated with liposomal curcumin (Figure 7B) consistent with the reduced tissue injury demonstrated in this group. The effect of liposomal curcumin on chemokine and cytokine mRNA expression *in vivo* after renal IR injury was investigated. TNF-α (Figure 7C), CCL5 (RANTES; Figure 8B), CCL2 (MCP-1, Figure 8C) and CXCL2 (MIP-2α, Figure 8D) were all reduced in curcumin-treated mice. These data are consistent with the described inhibition of MAPK by curcumin (Kim *et al.*, 2005) central to the activation of NF-κB and pro-inflammatory cytokine production (Jaswal *et al.*, 2007; Furuichi *et al.*, 2008).

A

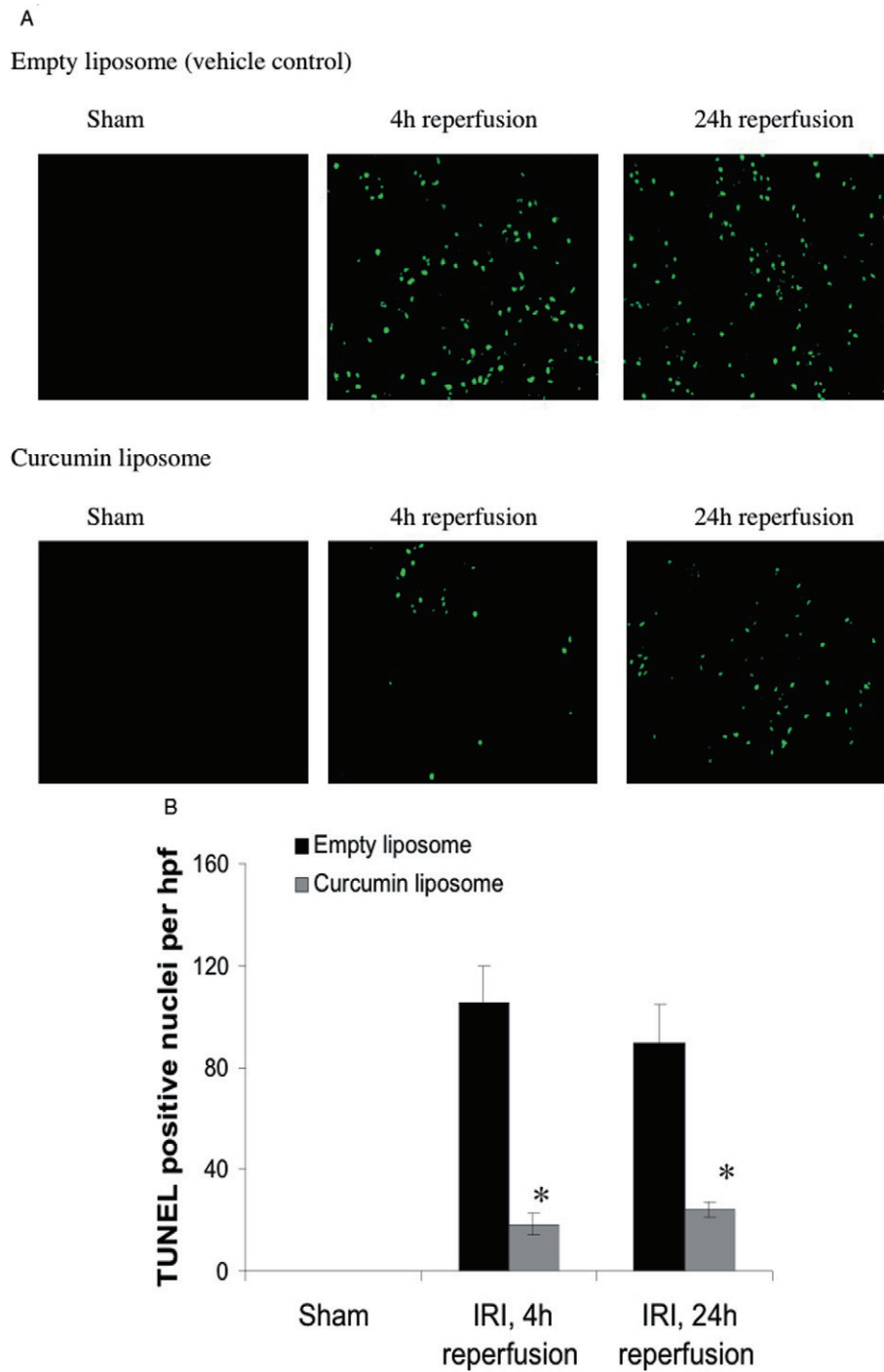Empty liposome (vehicle control)

B

Figure 6

Liposomal curcumin reduces TEC apoptosis following renal IR injury (IRI). (A) Representative fluorescent photomicrographs of kidney sections illustrating apoptotic nuclei (TUNEL fluorescent stain), representative of six sections per group (original magnification 200×). (B) Apoptotic tubular cells in kidneys from mice pretreated with curcumin liposome and vehicle control (empty liposomes) after renal IR injury or sham operation. Data are mean ± SEM of six mice per group. *$P < 0.05$, significant effect of curcumin liposomes.

Liposomal curcumin reduces renal neutrophil infiltration following IR injury

Polymorphonuclear leukocytes are a distinct infiltrating cell population in renal IR injury. Light microscopic assessment of haematoxylin and eosin (H&E) sections showed reduced neutrophil infiltration in mice pretreated with curcumin liposomes at both 4 and 24 h reperfusion (Figure 8A), in keeping with the known anti-inflammatory effect of curcumin (Srivastava, 1989; Ramsewak *et al.*, 2000).
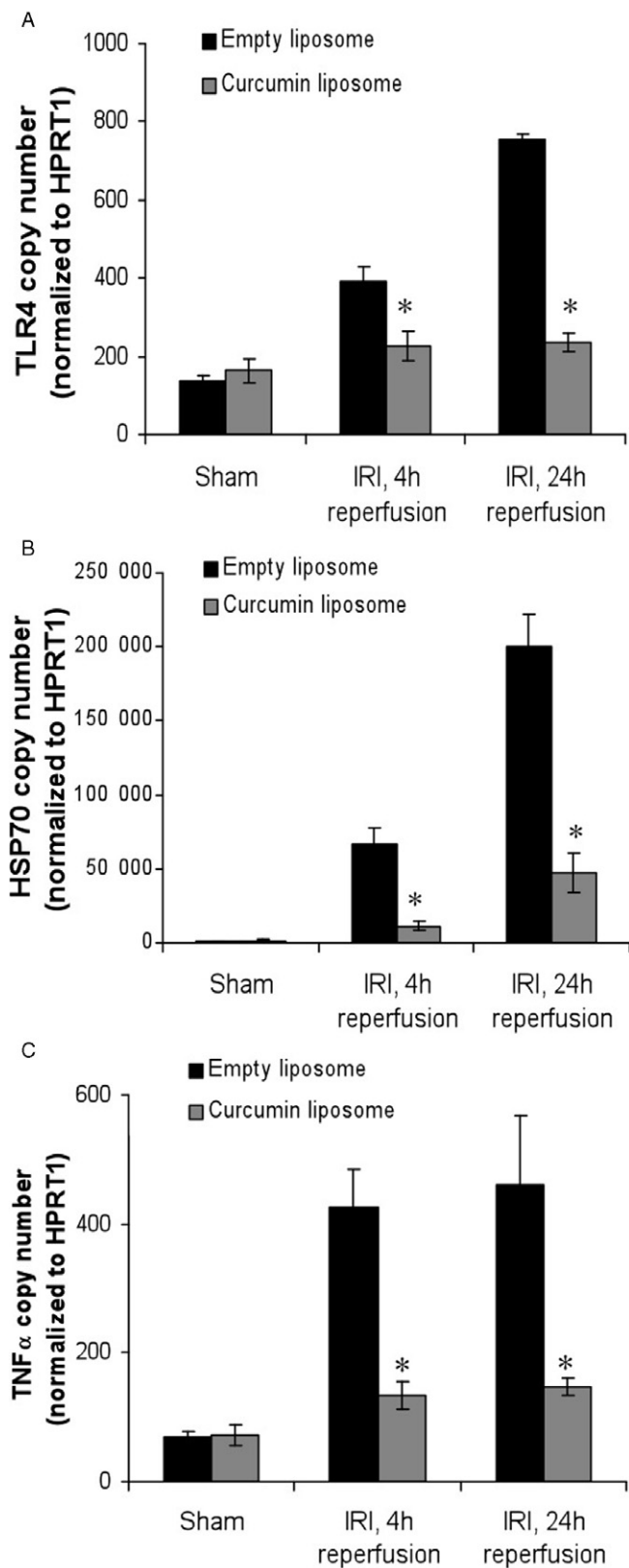
A

B

C

cellular injury. To assess whether the renoprotective effect of curcumin could be attributed to a reduction in the production of ROS, intracellular generation of O_2^- was visualized with the fluoroprobe DHE. DHE, freely permeable to cells, is oxidized on reaction with O_2^- to ethidium bromide (EtBr), which is trapped by intercalating with nuclear DNA and fluoresces red. Using confocal microscopy, tissue sections from mice treated with empty liposomes showed a widespread and marked increase in fluorescence (Figure 9A). Mice pretreated with curcumin liposomes demonstrated significantly reduced fluorescence at the same reperfusion time points. Concurrent measurement of superoxide dismutase (SOD) mRNA expression, the main enzyme responsible for dismutation of O_2^-, was up-regulated in curcumin-treated mice (Figure 9B).

The combination of O_2^- with resident NO forms peroxynitrite (ONOO-), which is capable of aggravating cellular damage by nitration of protein tyrosine residues. Fluorescent staining for 3-nitrotyrosine demonstrated marked protein nitration in TEC from mice receiving vehicle alone, which was reduced in mice receiving liposomal curcumin (Figure 10A). Western blot analysis of kidney tissue indicated the presence of a nitrated protein band at ~47 kDa (Figure 10B). These results confirm that protein nitration was significant in the vehicle-treated mice at both 4 and 24 h reperfusion. Oxidative stress also increases inducible NOS (iNOS), which aggravates tubular injury by supplying NO for peroxynitrite formation. mRNA expression for iNOS was significantly attenuated in mice pretreated with liposomal curcumin (Figure 10C), but only at 24 h; expression at 4 h did not reach statistical significance ($P = 0.08$).

The thioredoxin-interacting protein (TXNIP) functions as an inhibitor of the cellular antioxidant thioredoxin by binding to redox-active cysteine residues, thus promoting intracellular oxidative stress (Junn et al., 2000; Yamawaki and Berk, 2005). To verify expression of TXNIP in ischaemic renal tissue, we used immunofluorescence, Western blot analysis and RT-PCR. Figure 11A–C demonstrates up-regulation of TXNIP protein and mRNA that was most marked at 24 h reperfusion and ameliorated by pretreatment with curcumin liposomes.

Liposomal curcumin limits oxidative and nitrosative stress following IR injury

IR injury is associated with increased production of ROS, particularly superoxide (O_2^-), which is a major mediator of

Discussion

The major findings of this study are (i) liposomes encapsulating the lipophilic NF-κB inhibitor curcumin provided
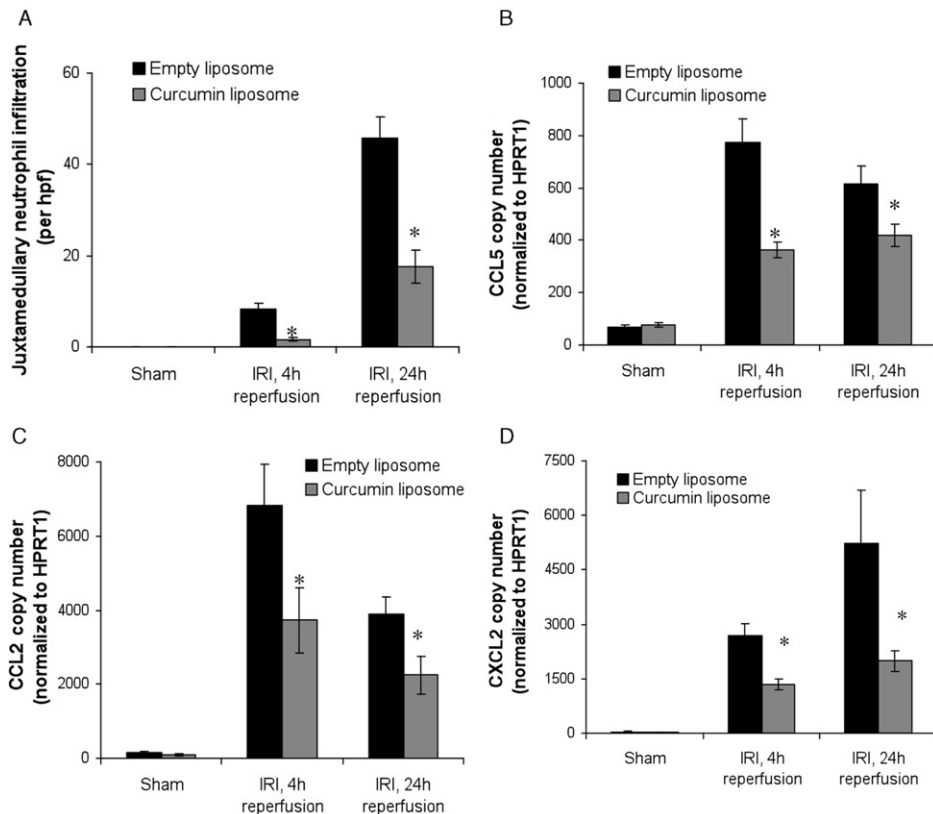
Figure 8

Liposomal curcumin reduces neutrophil infiltration and pro-inflammatory chemokine expression following renal IR injury (IRI). (A) Leukocyte influx in kidneys from mice pretreated with curcumin liposomes (grey bars) or vehicle control (black bars) 4 and 24 h after IR injury or sham operation. The number of neutrophils counted in 10 randomly selected high-power fields of corticomedulla (original magnification 400×), were significantly lower in mice receiving curcumin liposomes. RT-PCR was used to quantify mRNA expression of (B) CCL5, (C) CCL2 and (D) CXCL2. High expression of all chemokine factors was observed in IR injury of kidneys of mice treated with control vehicle (empty liposomes), when compared with mice receiving liposomal curcumin or sham-operated mice. Data are mean ± SEM of 10 mice per group. *$P < 0.05$, significant effect of curcumin liposomes.

targeted drug delivery to both renal TEC and APC; (ii) curcumin delivered to cells in this manner retained biological activity inhibiting nuclear up-regulation of p50 and p65 subunits of NF-kB, in addition to MAPK and phospho-S6RP expression; and (iii) conferred effective protection against renal IR injury. Liposomal curcumin resulted in substantial salvage of biochemical parameters, improved histological features, reduced neutrophil infiltration and a concomitant decrease in pro-inflammatory cytokine and chemokine expression. A major component of renal cytoprotection was mediated via decreased oxidative and nitrosative stress. For the first time, we demonstrated up-regulation of TXNIP in renal IR injury and a reduction in its expression following administration of liposomal curcumin.

To induce protection from IR injury, the cytoprotective agent must be delivered to renal TEC that represent the main site of oxidative stress and damage. Microscopy demonstrated these cells avidly endocytosed liposomal curcumin (Supplemental Figure S1 and 2), and subsequent studies of renal histology (Figure 5), cellular apoptosis (Figure 6) and oxidant stress (Figures 9–11) indicate that renal parenchyma was significantly protected from many aspects of IR injury

pathophysiology. Resident renal APC, macrophages and particularly DC (Dong *et al.*, 2005; 2007), are also implicated in reperfusion-related damage by generating pro-inflammatory cytokines. Inhibition of NF-κB activation and reduced production of TNF-α, CXCL2 and CCL2 (Figures 1 and 8, respectively) demonstrates decreased ability of APC to respond to IR injury-mediated stimuli. We have also shown previously that APC isolated following *in vivo* exposure to liposomal curcumin fail to up-regulate co-stimulatory molecule expression following a maturation stimulus (Rogers *et al.*, 2010a).

Oxygen-derived free radicals formed following IR injury aggravate tissue damage by protein and lipid oxidation. The oxygen radical scavenger SOD protects against renal parenchymal damage, and its expression is up-regulated by curcumin (Figure 9B), attenuating intracellular superoxide formation (Figure 9A). This correlates with previous studies demonstrating increased total SOD activity (Shen *et al.*, 2007). NO also influences widespread physiological processes and can be generated by three NOS isoforms (neuronal, endothelial and inducible). iNOS-generated NO contributes to IR pathophysiology by facilitating peroxynitrite production, and this
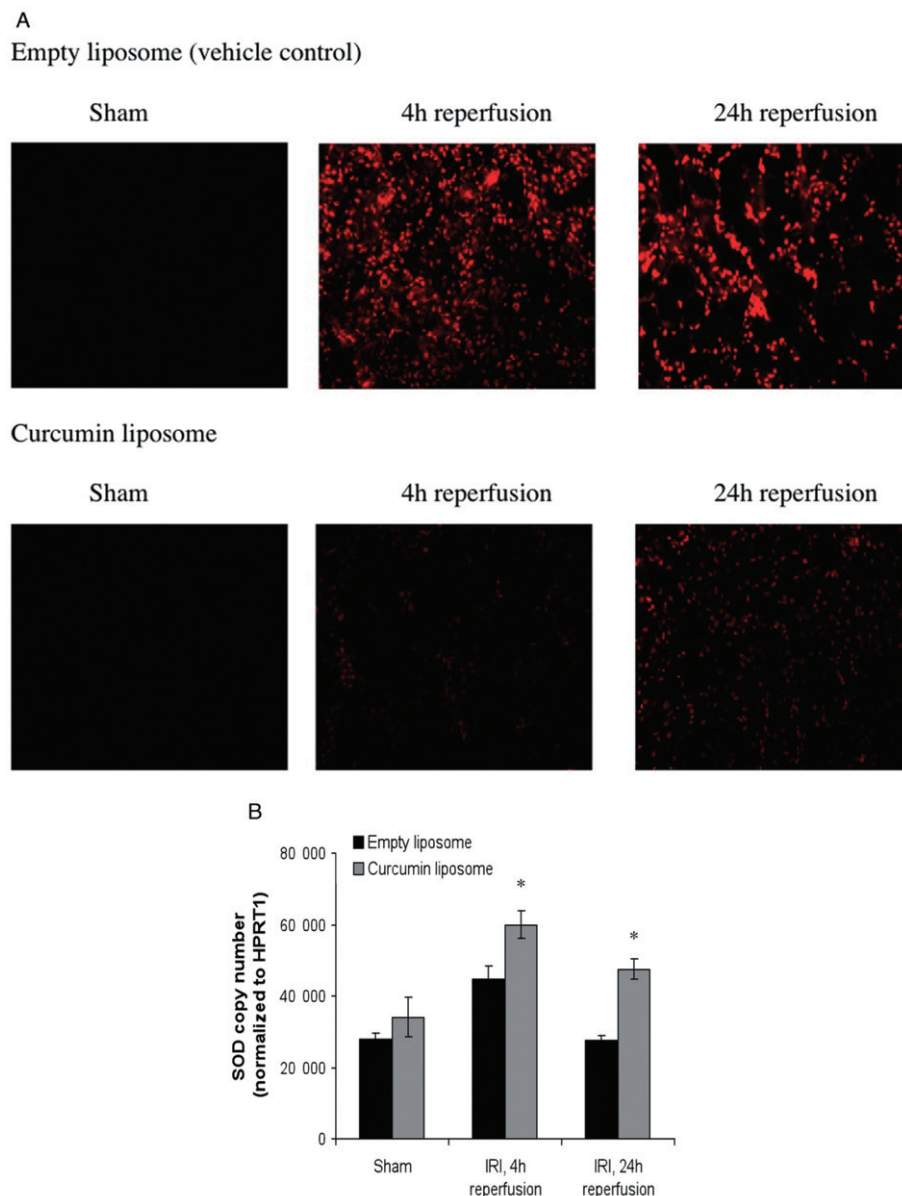
A

Empty liposome (vehicle control)

B

Figure 9

Liposomal curcumin reduces oxidative stress following renal IR injury (IRI). (A) Pretreatment with curcumin liposomes before renal IR injury reduced the amount of intracellular superoxide when compared with vehicle control at 4 and 24 h reperfusion after IR injury as shown by immunofluorescence. Photomicrographs are representative of six sections per group (original magnification 200×). (B) Renal tissue SOD gene expression was assessed by RT-PCR. SOD mRNA was significantly increased by pretreatment with curcumin liposome at 4 and 24 h after renal IR injury, compared with both sham operated mice and mice pretreated with vehicle control (empty liposomes). Data are mean ± SEM. *$P < 0.05$, significantly different from vehicle control; curcumin liposome + IR injury significantly different from curcumin liposome + sham.

process was effectively down-regulated by curcumin pretreatment (Figure 10A–C). TXNIP is up-regulated by IR injury (Figure 11) and promotes oxidative stress by inhibiting thioredoxin function and shifting intracellular redox stress. Previous *in vivo* studies have localized TXNIP up-regulation to dilated tubules in a model of diabetic nephropathy (Qi *et al.*, 2007; Advani *et al.*, 2009). Curcumin reduced renal tubular TXNIP protein and mRNA expression, providing an additional and previously undescribed antioxidant mechanism that contributed to the protective effect against IRI.

Curcumin possesses numerous pharmacological properties; its biological activity arises from the inhibition of signal transduction pathways, particularly (although not exclusively) direct suppression of NF-κB activity. Mechanisms include prevention of DNA-binding activity, decreased nuclear translocation of RelA (Jobin *et al.*, 1999), p65 (Kim *et al.*, 2005) or p50 subunits (as shown in Figure 1 in this study), inhibition of IκKα phosphorylation (Singh and Aggarwal, 1995) or degradation of IκBα (Jobin *et al.*, 1999). Suppression of NF-κB activation also occurs via other signal
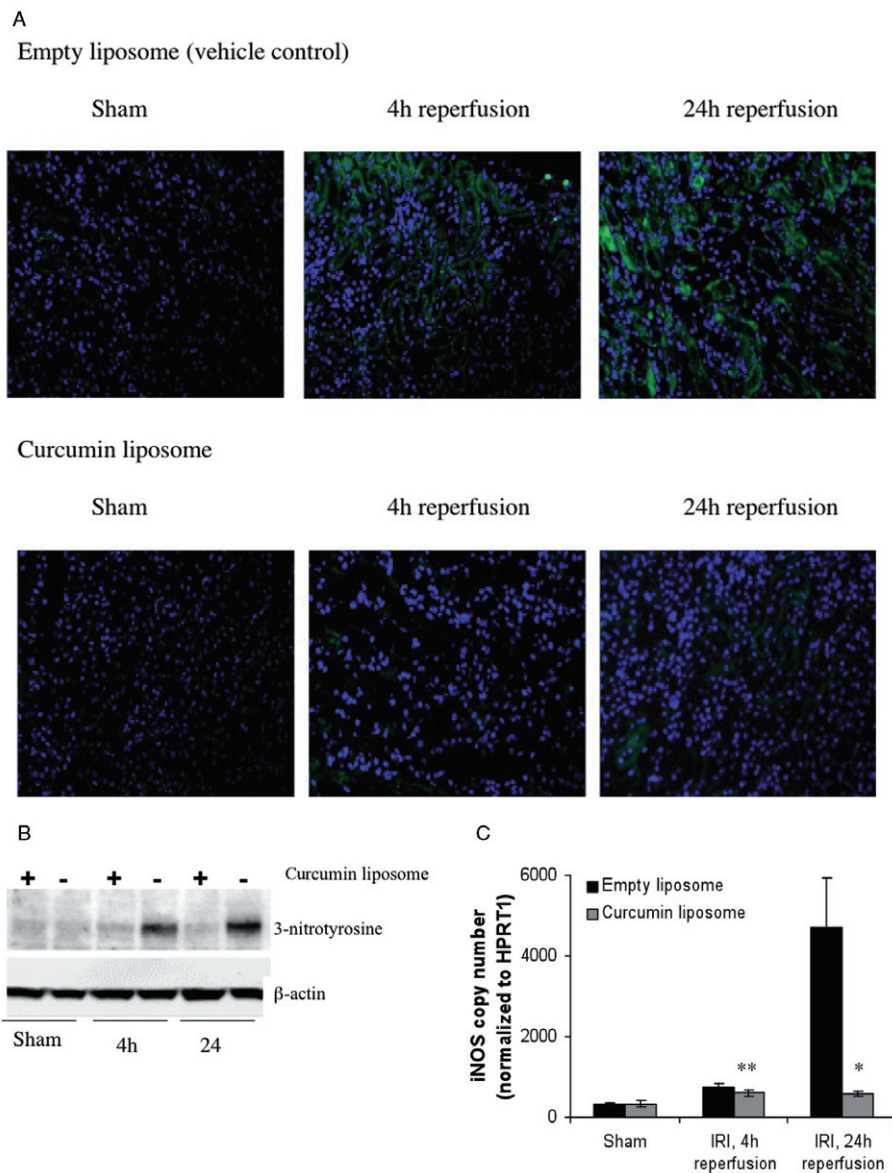
Figure 10

Liposomal curcumin reduces nitrosative stress following renal IR injury (IRI). (A) Pretreatment with curcumin liposomes before renal IR injury reduced the amount of protein tyrosine nitration when compared with vehicle control at 4 and 24 h reperfusion after IR injury, as shown by immunofluorescence. Photomicrographs are representative of six sections per group (original magnification 200×). (B) Pretreatment with curcumin liposomes before renal IR injury reduced the amount of protein tyrosine nitration when compared with vehicle control at 4 and 24 h reperfusion after IR injury as shown by immunoblotting. 3-Nitrotyrosine is detected at ~47 kDa. The figure is representative of three independent experiments. (C) Renal tissue iNOS gene expression was assessed by RT-PCR. iNOS mRNA was up-regulated by IR injury at both 4 and 24 h after renal IR injury, compared with both sham operated mice and mice pretreated with curcumin liposomes, although the effect was only significantly different at 24 h reperfusion. Data are mean $\pm$ SEM. *$P < 0.05$; **$P = 0.08$, significant effect of curcumin liposomes.

transduction pathways, and we have demonstrated inhibition of both pS6RP, the downstream target of the Akt signalling cascade and p42/44 MAPK (Figure 3). Curcumin is also an inhibitor of the transcription activator AP-1 (via JNK), Wnt/ β-catenin (Leow *et al.*, 2010), mammalian target of rapamycin (Beevers *et al.*, 2006) and phosphorylase kinase (Reddy and Aggarwal, 1994; Heng, 2000; Heng, 2010). Inhibition of phosphorylase kinase, by virtue of its ability to modify binding site specificity and affect both tyrosine and

serine/threonine kinases, has been proposed as a unifying mechanism to explain the multiple modes of action of curcumin (Yuan *et al.*, 1993; Heng, 2010).

There is an increasing body of work employing strategies to prevent or treat IR injury, ranging from ischaemic preconditioning (Jamieson and Friend, 2008, Lutz *et al.*, 2010), to blockade of cytokines and chemokines (Lutz *et al.*, 2005; Rusai *et al.*, 2008) and over-expression of protective genes (Lutz *et al.*, 2008). Delivery methods vary (direct infusion
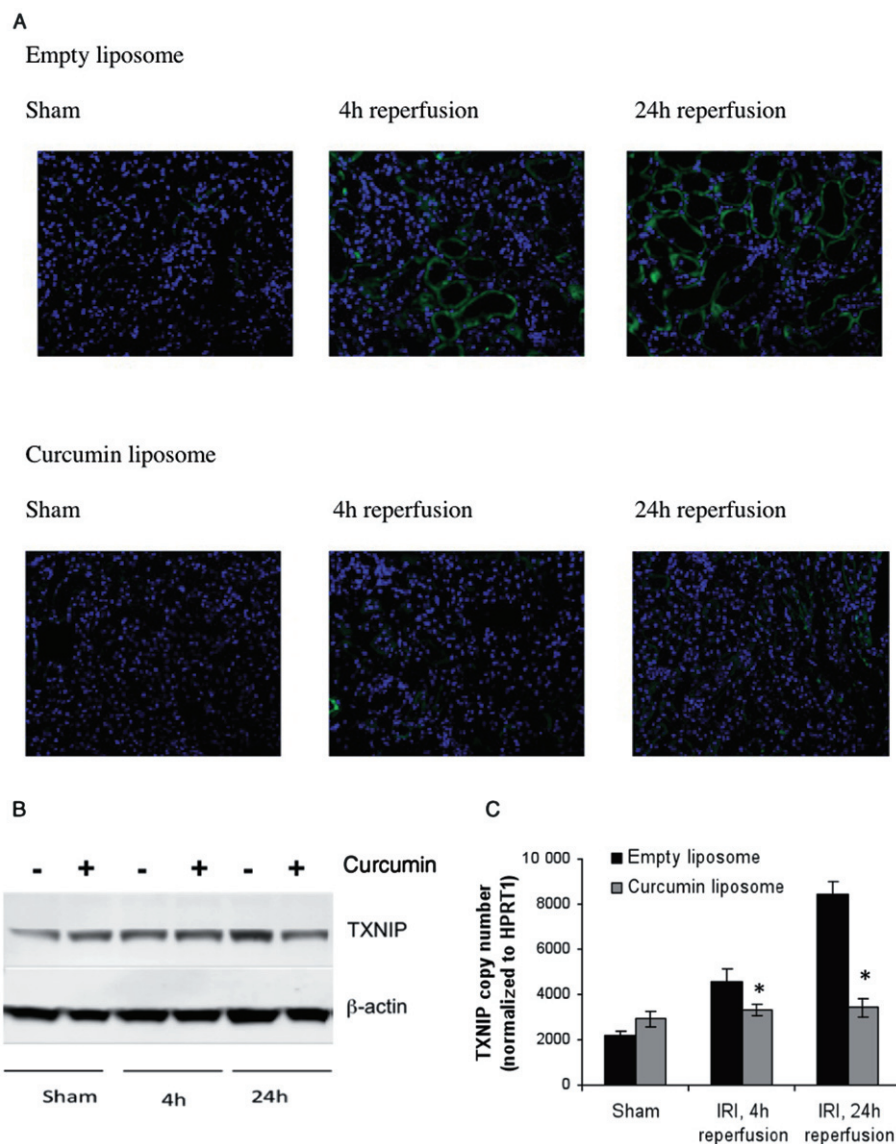
Figure 11

Renal IR injury (IRI) up-regulates TXNIP expression that is ameliorated by liposomal curcumin. (A) IR injury up-regulated TXNIP expression at 4 and 24 h reperfusion, and this expression was ameliorated by pretreatment with liposomal curcumin, as shown by immunofluorescence. Photomicrographs are representative of six sections per group (original magnification 200×). (B) Pretreatment with curcumin liposomes before renal IR injury reduced the amount of TXNIP protein expression when compared with vehicle control at 24 h reperfusion after IR injury as shown by immunoblotting. TXNIP is detected at 46 kDa. The figure is representative of three independent experiments. (C) Renal parenchymal TXNIP gene expression was up-regulated by IR injury at both 4 and 24 h after renal IR injury, compared with both sham operated mice and mice pretreated with curcumin liposomes. Data are mean ± SEM. *$P < 0.05$, significant effect of curcumin liposomes.

into the vascular tree, adenoviral infection) but lack immediate clinical applicability. NF-κB plays a central role in the initiation and progression of IR injury. It exists as dimers from a family of five different proteins [p50, p52, p65 (RelA), RelB and c-Rel]; the predominant form is a heterodimer of p50 and p65 proteins sequestered in the cytosol with inhibitory proteins preventing nuclear translocation. A significant feature of NF-κB in IR injury is the large number of regulated genes and its central role in the cytotoxic and inflammatory cascade. Blockade of the NF-κB signalling pathway provides an opportunity for novel therapeutic strategies. Adenoviral

mediated over-expression of IκBα has led to decreased NF-κB DNA-binding activity ameliorating IR injury and/or graft rejection (Bach et al., 1997; Bradham et al., 1999, Taylor et al., 1999). Perfusion of allogeneic rat kidneys with NF-κB oligodeoxynucleotide prior to transplantation abolished NF-κB activity in vivo and inhibited inflammatory responses (Vos et al., 2000). Salvage of renal function using liposomal curcumin in our study compares favourably with reports of other NF-κB inhibitors. Additionally, our model provides effective delivery and a breadth of cytoprotective effects not demonstrated by other agents.

Curcumin is hydrophobic and cannot be administered systemically without modification; oral bioavailability is limited by significant hepatic metabolism (Ireson *et al.*, 2002). Liposomal encapsulation of curcumin used in this study offers targeted cellular delivery of therapy, flexibility in administration and safety. Its lipophilicity ensures high liposome entrapment efficiency and incorporation of curcumin within a lipid carrier also protects it from enzyme degradation *in vivo*. The use of liposomes exploits the phagocytic capacity of APC and TEC, as well as curcumin's immunomodulatory, anti-inflammatory and antioxidant properties. The total administered dose of curcumin was in keeping with dosing from previous studies (Capini *et al.*, 2009) and doses used for effective treatment of malignancy in rodent models (Lan *et al.*, 2005; Wang *et al.*, 2008, Mach *et al.*, 2009) but was substantially lower than the oral doses required to produce pharmacologically significant plasma levels (Lao *et al.*, 2006; Bayrak *et al.*, 2008). Cellular endocytosis of curcumin liposomes did not induce obvious cytotoxicity or adverse events in treated mice at this dose.

In conclusion, this study demonstrates that liposomal curcumin can provide targeted cellular delivery to renal TEC and APC *in vivo*, conferring protection from IR injury, mediated by NF-κB. Liposomal endocytosis of this cytoprotective agent by both cell compartments is advantageous in IRI. Renal TEC are the main site of hypoxic damage and oxidative stress following IR injury, and resident APC mediate the innate immune response to parenchymal injury. Protective mechanisms are regulated through multiple pathways, including inhibition of apoptosis and neutrophil recruitment, enhanced antioxidant enzyme expression, reduced NO generation and diminished TXNIP expression. These data were observed in a model of severe ischemic renal injury at two discrete, acute reperfusion time points. Assessment of the effect of liposomal curcumin on longer-term outcomes following IR injury is also required, but reperfusion times were curtailed in the current study for humane reasons. This treatment has potential clinical application to improve outcomes in the setting of surgical procedures that affect organ perfusion.

Acknowledgements

Conflict of interest

The authors declare no conflict of interest.

References

Advani A, Gilbert R, Thai K, Gow R, Langham R, Christensen P *et al.* (2009). Expression, localization, and function of the thioredoxin system in diabetic nephropathy. J Am Soc Nephrol 20: 730–741.

Agwarwal B, Kumar A, Bharti A (2003). Anticancer potential of curcumin: preclinical and clinical studies. Anticancer Res 23: 363–398.

Apisariyakul A, Vanittanakom N, Buddhasukh D (1995). Antifungal activity of turmeric oil extracted from Curcuma longa (Zingiberaceae). J Ethnopharmacol 49: 163–169.

Bach FH, Ferran C, Soares M, Wrighton CJ, Anrather J, Winkler H *et al.* (1997). Modification of vascular responses in xenotransplantation: inflammation and apoptosis. Nat Med 3: 944–948.

Balasubramanyam M, Koteswari A, Kumar R, Monickaraj S, Maheswari J, Mohan V (2003). Curcumin-induced inhibition of cellular reactive oxygen species generation: novel therapeutic implications. J Biosci 28: 715–721.

Bayrak O, Uz E, Turgut F, Atmaca A, Sahin S, Yildirim M *et al.* (2008). Curcumin protects against ischemia/reperfusion injury in rat kidneys. World J Urol 26: 285–291.

Beevers C, Li F, Liu L, Huang S (2006). Curcumin inhibits the mammalian target of rapamycin-mediated signaling pathways in cancer cells. Int J Cancer 119: 757–764.

Boros P, Bromberg J (2006). New cellular and molecular immune pathways in ischemia-reperfusion injury. Am J Transplant 6: 652–658.

Bradham CA, Schemmer P, Stachlewitz RF, Thurman RG, Brenner DA (1999). Activation of nuclear factor-kappaB during orthotopic liver transplantation in rats is protective and does not require Kupffer cells. Liver. Transpl Surg 5: 282–293.

Capini C, Jaturanpinyo M, Chang H-I, Mutalik S, Mcnally A, Street S *et al.* (2009). Antigen-specific suppression of inflammatory arthritis using liposomes. J Immunol 182: 3556–3565.

Chen Y, Tan T (1998). INhibition of the c-jun N-terminal kinase (JNK) siganling pathway by curcumin. Oncogene 17: 173–178.

Choudhuri T, Pal S, Agwarwal M, Das T, Sa G (2002). Curcumin induces apoptosis in human breast cancer cells through p53-dependent Bax induction. FEBS Lett 512: 334–340.

Dong X, Swaminathan S, Bachman L, Croatt A, Nath K, Griffin M (2005). Antigen presentation by dendritic cells in renal lymph nodes is linked to systemic and local injury to the kidney. Kidney Int 68: 1096–1108.

Dong X, Swaminathan S, Bachman L, Croatt A, Nath K, Griffin M (2007). Resident dendritic cells are the predominant TNF-secreting cell in early renal ischaemia-reperfusion injury. Kidney Int 71: 619–628.

Donnahoo K, Meldrum D, Shenkar R, Chung C, Abraham E, Harken A (2000). Early renal ischemia, with or without reperfusion, activates NF kappa B and increases TNF-alpha bioactivity in the kidney. J Urol 163: 1328–1332.

Feldman H, Gayner R, Berlin J, Roth D, Silibovsky R, Krushner S *et al.* (1996). Delayed graft function reduces renal allograft survival independent of acute rejection. Nephrol Dial Transplant 11: 1306–1313.

Furuichi W, Wada T, Kaneko S, Murphy P (2008). Roles of chemokines in renal ischemia/reperfusion injury. Front Biosci 13: 4021–4028.

Garg A, Buchholz T, Aggarwal B (2005). Chemosensitization and radiosensitization of tumours by plant polyphenols. Antioxid Redox Signal 7: 1630–1647.

Halloran P, Homik J, Goes N, Lui S, Urmson J, Ramassar V et al. (1997). The 'injury response': a concept linking nonspecific injury, acute rejection, and long-term transplant outcomes. Transplant Proc 29: 79–81.

Heng M (2010). Curcumin targeted signaling pathways: basis for anti-photoaging and anti-carcinogenic therapy. Int J Dermatol 49: 608–622.

Heng M, Song M, Harker J, Heng M (2000). Drug-induced suppression of phosphorylase kinase activity correlates with resolution of psoriasis as assessed by clinical, histological and immunological parameters. Br J Dermatol 143: 937–949.

Hetzel G, Klein B, Brause M, Westhoff A, Willers R, Sandmann W et al. (2002). Risk factors for delayed graft function on the long-term outcome of renal transplantation. Transpl Int 15: 10–16.

Ireson C, Jones D, Orr S, Coughtrie M, Boocock D, Williams M et al. (2002). Metabolism of the cancer chemopreventive agent curcumin in human and rat intestine. Cancer Epidemiol Biomarkers Prev 11: 105–111.

Jagetia G, Aggarwal B (2007). Spicing up the immune system by curcumin. J Clin Immunol 27: 19–35.

Jamieson R, Friend P (2008). Organ reperfusion and preservation. Front Biosci 13: 221–235.

Jaswal J, Gandhi M, Finegan B, Dyck J, Clanachan A (2007). Inhibition of p38 MAPK and AMPK restores adenosine-induced cardioprotection in heart stressed by antecedent ischemia by altering glucose utilization. Am J Physiol Heart Circ Physiol 293: H1107–H1114.

Jobin C, Bradham C, Russo M, Juma B, Narula A, Brenner D et al. (1999). Curcumin blocks cytokine-mediated NF-κB activation and proinflammatory gene expression by inhibiting inhibitory factor I-κB kinase activity. J Immunol 163: 3474–3483.

Junn E, Han S, Im J, Yang Y, Cho E, Um H et al. (2000). Vitamin D3 up-regulated protein 1 mediates oxidative stress via suppressing tioredoxin function. J Immunol 164: 6287–6295.

Kim G, Kim K, Lee S, Yoon M, Lee H, Moon D et al. (2005). Curcumin inhibits immunostimulatory function of dendritic cells: MAPKs and translocation of NF-kB as potential targets. J Immunol 174: 8116–8124.

Lan L, Braiteh F, Kurzrock R (2005). Liposom-encapsulated curcumin. Cancer 104: 1322–1331.

Lao C, Ruffin M, Normolle D, Heath D, Murray S, Bailey J et al. (2006). Dose escalation of a curcuminoid formulation. BMC Complement Altern Med 6: 10.

Leemans J, Stokman G, Claessen N, Rouschop K, Teske G, Kirschning C et al. (2005). Renal-associated TLR2 mediates ischemia/reperfusion injury in the kidney. J Clin Invest 115: 2894–2903.

Leow P, Tian Q, Ong Z, Yang Z, Ee P (2010). Antitumor activity of natural compounds, curcumin and PKF118-310, as Wnt/beta-catenin antagonists against human osteosarcoma cells. Invest New Drugs 28: 766–782.

Lutz J, Tyao Y, Song E, Antus B, Hamar P, Liu S et al. (2005). Inhibition of matrix metalloproteinases during chronic allograft nephropathy in rats. Transplantation 79: 655–661.

Lutz J, Luong IA, Strobl M, Deng M, Huang H, Anton M et al. (2008). The A20 gene protects kidneys from ischemia/reperfusion injury by suppressing pro-inflammatory activation. J Mol Med 86: 1329–1339.

Lutz J, Thürmel K, Heeman U (2010). Anti-inflammatory treatment strategies for ischemia/repefusion injury in transplantation. J Inflamm (Lond) 7: 27–34.

Mach CM, Mathew L, Mosley SA, Kurzrock R, Smith JA (2009). Determination of minimum effective dose and optimal dosing schedule for liposomal curcumin in a xenograft human pancreatic cancer model. Anticancer Res 29: 1895–1899.

Mazumder A, Raghavan K, Weinstein J, Kohn K, Pommier Y (1995). Inhibition of human immunodeficiency virus type-1 integrase by curcumin. Biochem Pharmacol 49: 1165–1170.

Negi P, Jayaprakasha G, Jagan Mohan Rao L, Sakariah K (1999). Antibacterial activity of turmeric oil: a byproduct from curcumin manufacture. J Agric Food Chem 47: 4297–4300.

Preston R, Epstein M (1997). Ischemic renal disease: an emerging cause of chronic renal failure and end-stage renal failure. J Hypertens 15: 1365–1377.

Qi W, Chen X, Gilbert R, Zhang Y, Waltham M, Schache M et al. (2007). High glucose-induced thioredoxin interacting protein in renal proximal tubule cells is independent of transforming growth factor-β1. Am J Pathol 171: 744–754.

Ramsewak R, Dewitt D, Nair M (2000). Cytotoxicity, antioxidant and anti-inflammatory activities of curcumins I-III from Curcuma longa. Phytomedicine 7: 303–308.

Reddy S, Aggarwal B (1994). Curcumin is a non-competitive and selective inhibitor of phosphorylase kinase. FEBS Lett 341: 19–22.

Rogers N, Kireta S, Coates P (2010a). Curcumin generates maturation-resistant dendritic cells and regulatory T-cells in vitro and in vivo. Immunol Cell Biol 88: A24.

Rogers N, Kireta S, Coates P (2010b). Curcumin induces maturation-arrested dendritic cells and expands regulatory T-cells in vivo and in vitro. Clin Exp Immunol 162: 460–473.

Ruby A, Kuttan G, Babu K, Rajasekharan K, Kuttan R (2003). Anti-tumor and antioxidant activity of natural curcuminoids. Cancer Lett 94: 79–83.

Rusai K, Huang H, Sayed N, Strobl M, Roos M, Schmaderer C et al. (2008). Administration of interleukin-1 receptor antagonist ameliorates renal ischemia-reperfusion injury. Transpl Int 21: 572–580.

Shen S, Zhang Y, Xiang J, Xiong C (2007). Protective effect of curcumin against liver warm ischemia/reperfusion injury in rat model is associated with regulation of heat shock protein and antioxidant enzyme. World J Gastroenterol 13: 1953–1961.

Shoskes D, Halloran P (1996). Delayed graft function in renal transplantation: etiology, management and long-term significance. J Urol 75: 82–87.

Singh S, Aggarwal B (1995). Activation of transcription factor NF-kB is suppressed by curcumin (diferuloylmethane). J Biol Chem 270: 24995–25000.

Srivastava R (1989). Inhibition of neutrophil response by curcumin. Agents Actions 28: 298–303.

Taylor BS, Shao L, Gambotto A, Ganster RW, Geller DA (1999). Inhibition of cytokine-induced nitric oxide synthase expression by gene transfer of adenoviral I kappa B alpha. Surgery 126: 142–147.

Tsoulfas G, Geller D (2001). NF-κB in transplantation: friend or foe? Transpl Infect Dis 3: 212–219.

Vos I, Govers R, Gröne H, Kleij L, Schurink M, De Weger R et al. (2000). NFkappaB decoy oligodeoxynucleotides reduce monocyte infiltration in renal allografts. FASEB J 14: 815–822.

Wang D, Veena M, Stevenson K, Tang C, Ho B, Suh J *et al*. (2008). Liposome-encapsulated curcumin suppresses growth of head and neck squamous cell carcinoma in vitro and in xenografts through the inhibition of nuclear factor ?B by an AKT-independent pathway. Clin Cancer Res 14: 6228–6236.

Wu H, Chen G, Wyburn K, Yin J, Bertolino P, Eris J *et al*. (2007). TLR4 activation mediates kidney ischemia/reperfusion injury. J Clin Invest 117: 2847–2859.

Yadav V, Mishra K, Singh D, Mehrotra S, Singh V (2005). Immunomodulatory effects of curcumin. Immunopharmacol Immunotoxicol 27: 485–497.

Yamawaki H, Berk B (2005). Thioredoxin: a multifunctional antioxidant enzyme in kidney, heart and vessels. Curr Opin Nephrol Hypertens 14: 149–153.

Yuan C, Huang C, Graves D (1993). Phosphorylase kinase: a metal ion-dependent dual specificity kinase. J Biol Chem 268: 17683–17686.

Supporting information

Additional Supporting Information may be found in the online version of this article:

Figure S1 DiI-labelled liposomes are endocytosed by renal tubular epithelial cells. Twenty-four hours after injection, kidneys of C57BL/6 mice injected i.v. with (a) PBS or (b) DiI-labelled (red fluorescent) liposomes were removed and snap frozen in OCT. Sections of frozen kidney were stained with DAPI as shown (original magnification 200×). Liposomes located to renal tubular epithelial cells (Figures 1B, G = glomerulus, T = tubule).

Figure S2 DiI-labelled liposomes are endocytosed by macrophages and DC. Twenty-four hours after injection, kidneys of C57BL/6 mice injected i.v. with (a) PBS or (b) DiI-labelled (red fluorescence) liposomes were removed and digested. Isolated APC were stained with anti-CD11b FITC, anti-CD11c FITC or PE-CY7, anti-F480 PE-CY5, anti-CD8a APC, anti-B220 PE-CY5, anti-PDCA FITC, or anti-MHC APC and analysed by flow cytometry. Red fluorescent cells were gated as shown (P2) and appear black in each plot. Results are representative of three independent experiments.

Please note: Wiley-Blackwell are not responsible for the content or functionality of any supporting materials supplied by the authors. Any queries (other than missing material) should be directed to the corresponding author for the article.